Free Radical Biology & Medicine 51 (2011) 464–473

Contents lists available at ScienceDirect

Free Radical Biology & Medicine

journal homepage: www.elsevier.com/locate/freeradbiomed

Original Contribution

Oxidizing substrate specificity of *Mycobacterium tuberculosis* alkyl hydroperoxide reductase E: kinetics and mechanisms of oxidation and overoxidation

Aníbal M. Reyes [a,b], Martín Hugo [a,b], Andrés Trostchansky [a,b], Luciana Capece [c], Rafael Radi [a,b], Madia Trujillo [a,b,*]

[a] Departamento de Bioquímica, Universidad de la República, 11800 Montevideo, Uruguay
[b] Center for Free Radical and Biomedical Research, Universidad de la República, 11800 Montevideo, Uruguay
[c] Departamento de Química Inorgánica, Analítica y Química Física/INQUIMAE-CONICET, Facultad de Ciencias Exactas y Naturales, Universidad de Buenos Aires, Buenos Aires, Argentina

ARTICLE INFO

Article history:
Received 23 December 2010
Revised 7 April 2011
Accepted 12 April 2011
Available online 17 April 2011

Keywords:
Mycobacterium tuberculosis
Peroxiredoxin
Peroxidase
Hydroperoxide
Arachidonic acid
Alkyl hydroperoxide reductase E
Free radicals

ABSTRACT

Alkyl hydroperoxide reductase E (AhpE), a novel subgroup of the peroxiredoxin family, comprises *Mycobacterium tuberculosis* AhpE (*Mt*AhpE) and AhpE-like proteins present in many bacteria and archaea, for which functional characterization is scarce. We previously reported that *Mt*AhpE reacted ~10^3 times faster with peroxynitrite than with hydrogen peroxide, but the molecular reasons for that remained unknown. Herein, we investigated the oxidizing substrate specificity and the oxidative inactivation of the enzyme. In most cases, both peroxidatic thiol oxidation and sulfenic acid overoxidation followed a trend in which those peroxides with the lower leaving-group pK_a reacted faster than others. These data are in agreement with the accepted mechanisms of thiol oxidation and support that overoxidation occurs through sulfenate anion reaction with the protonated peroxide. However, *Mt*AhpE oxidation and overoxidation by fatty acid-derived hydroperoxides (~10^8 and 10^5 M^{-1} s^{-1}, respectively, at pH 7.4 and 25 °C) were much faster than expected according to the Brønsted relationship with leaving-group pK_a. A stoichiometric reduction of the arachidonic acid hydroperoxide 15-HpETE to its corresponding alcohol was confirmed. Interactions of fatty acid hydroperoxides with a hydrophobic groove present on the reduced *Mt*AhpE surface could be the basis of their surprisingly fast reactivity.

Mycobacterium tuberculosis, the causative agent of tuberculosis disease, is an extremely successful pathogen, responsible for near 2 million deaths per year (http://www.who.int/tb/publications/global_report/2010/en/index.html). The variable efficiency of available vaccines, the emergence of multi- and extensively drug-resistant strains, and the frequent co-infection with HIV have resulted in the immediate need to identify unique targets for new therapeutic approaches [1–4]. *M. tuberculosis* exhibits diverse strategies to survive inside the hostile environment of host cells [5–7]. Among them, the antioxidant defenses that allow the bacteria to detoxify reactive oxygen and nitrogen species formed by activated macrophages are under active investigation, because they could provide clues for rational drug development. Peroxynitrite and hydrogen peroxide (H_2O_2) are cytotoxic peroxides formed inside phagosomes upon macrophage activation [8–10]. These species, in turn, can participate in lipid peroxidation reactions through fatty acid-derived free radical production and propagation by autoxidation [11,12]. Lipid hydroperoxides can also be formed by enzymatic mechanisms through lipoxygenase-catalyzed reactions [13,14]. Fatty acid hydroperoxides are released from membranes by phospholipase A_2[15] and are cytotoxic for various microorganisms [16,17]. Indeed, peroxide detoxification is required for *M. tuberculosis* to survive in macrophages and to establish acute and persistent infections in animal tuberculosis models [18–20]. This is accomplished by heme-dependent and several thiol-dependent peroxidases of the peroxiredoxin (Prx) family. The catalase/peroxidase enzyme KatG [21] mediates isoniazid activation [22] and in pathogenic strains, its deficiency has been reported to be compensated for by overexpression of the Prx alkyl hydroperoxide reductase C [23]. A second *M. tuberculosis* peroxiredoxin, thioredoxin peroxidase, rapidly reduces H_2O_2 and peroxynitrite and seems to play a major role in infectivity [18,19]. The other Prxs codified by the *M. tuberculosis* genome are two bacterioferritin comigratory proteins and alkyl hydroperoxide reductase E (AhpE) [24].

Abbreviations: AhpE, alkyl hydroperoxide reductase E; BHT, butylated hydroxytoluene; 3-CPBA, 3-chloroperoxybenzoic acid; cumeneOOH, cumene hydroperoxide; DTPA, diethylenetriamine pentaacetic acid; DTNB, 5,5′-dithiobis-(2-nitrobenzoic acid); DTT, 1,4-dithiothreitol; arachidonic acid, 5*Z*,8*Z*,11*Z*,14*Z*-eicosatetraenoic acid; 15-HETE, (±)15-hydroxy-5*Z*,8*Z*,11*Z*,13*E*-eicosatetraenoic acid; 12-HETE-d8, 12*S*-hydroxy-5*Z*,8*Z*,10*E*,14*Z*-eicosatetraenoic-5,6,8,9,11,12,14,15-d8 acid; 15-HpETE, 15*S*-hydroperoxy-5*Z*,8*Z*,11*Z*,13*E*-eicosatetraenoic acid; α-linolenic acid, 9*Z*,12*Z*,15*Z*-octadecatrienoic acid; LOX, lipoxidase; C_P, peroxidatic cysteine; Prx, peroxiredoxin; *t*-BuOOH, *tert*-butylhydroperoxide.

* Corresponding author at: Departamento de Bioquímica and Center for Free Radical and Biomedical Research, Universidad de la República, General Flores 2125, 11800 Montevideo, Uruguay. Fax: +598 2 9249563.
E-mail address: madiat@fmed.edu.uy (M. Trujillo).

0891-5849/$ – see front matter © 2011 Elsevier Inc. All rights reserved.
doi:10.1016/j.freeradbiomed.2011.04.023

AhpE, which has been identified in the *M. tuberculosis* membrane fraction using a proteomics approach [25], is described as a one-cysteine Prx because it lacks a resolving cysteine. However, the structure and sequence of *Mt*AhpE show greater similarity with two-cysteine Prxs than with typical one-cysteine Prxs (http://peroxibase.toulouse.inra.fr/classes.php/[26] and http://www.csb.wfu.edu/prex/[27]). Moreover, some AhpE-like proteins, conserved among actinobacteria and some other bacteria and archaea, contain additional cysteine residues in their sequence whose contribution to catalysis has not been investigated so far. *Mt*AhpE transcription increases in models of the dormant phase of tuberculosis disease, indicating a regulated expression [28]. The crystallography structure of the enzyme has been resolved under reduced and oxidized states, with the peroxidatic cysteine (C_P) as thiol and sulfenic acid, respectively [29]. We have previously investigated the peroxidase activity of *Mt*AhpE [30], being the first Prx of the AhpE family to be functionally characterized. The physiological reducing substrate(s) for *Mt*AhpE (as well as other members of the AhpE class) is still unknown, but its catalytic activity was demonstrated using the artificial substrates dithiothreitol (DTT) and thionitrobenzoic acid [30]. The enzyme reduced peroxynitrite faster than H_2O_2 (1.9×10^7 versus $8.2\times10^4\ M^{-1}\ s^{-1}$ at pH 7.4 and 25 °C). This oxidizing substrate specificity is similar to what we reported for human peroxiredoxin 5, an atypical two-cysteine peroxiredoxin, but differs from what we and other groups have found for typical two-cysteine Prxs [31–34]. Taking advantage of the change in fluorescence intensity that occurred during *Mt*AhpE treatment with H_2O_2 in excess, we also reported the oxidative inactivation by C_P overoxidation ($40\ M^{-1}\ s^{-1}$ at pH 7.4 and 25 °C) [30]. The fact that *Mt*AhpE (a) forms a relatively stable sulfenic acid derivative upon oxidation, (b) presents a single cysteine residue per monomer, the C_P, and (c) changes intrinsic fluorescence properties upon C_P oxidation and overoxidation,[1] facilitating direct kinetic determinations, makes the enzyme a useful model to evaluate the catalytic and inactivation mechanisms for Prxs in general. Indeed, our previous work on *Mt*AhpE indicated that the mechanism of C_P overoxidation involves sulfenate (RSO^-) as the reactant species [30]:

$$C_P\ \text{oxidation}: RS^- + H_2O_2 \rightarrow RSOH + OH^-. \quad (1)$$

$$C_P\ \text{overoxidation}: RSO^- + H_2O_2 \rightarrow RSO_2H + OH^-. \quad (2)$$

Herein, we have investigated the oxidizing substrate specificity as well as the mechanism and kinetics of oxidative inactivation of AhpE from *M. tuberculosis*. Our results indicate that for most peroxides, oxidation as well as oxidative inactivation rates correlate with leaving-group pK_a, indicating that both reactions occur by similar mechanisms. In contrast, the hydroperoxide at position 15 of arachidonic acid (15-HpETE) as well as linolenic acid-derived hydroperoxides reacted surprisingly fast and the molecular mechanisms underlying this reactivity are proposed.

[1] This was confirmed by the lack of any change in fluorescence intensity when *Mt*AhpE mutated in C_P instead of the wild-type enzyme was used; by the linear dependency of the observed rate constant of the change in intrinsic *Mt*AhpE fluorescence with peroxide concentration, indicating that a bimolecular reaction between the oxidant and the enzyme was the rate-limiting step in the process leading to the change in fluorescence intensity during both enzyme oxidation and overoxidation; by the identification of sulfenic acid as the product of enzyme oxidation by equimolar concentrations of the oxidant by trapping it with monothiols such as GSH and *N*-acetylcysteine and detection of the corresponding mixed disulfides and the identification of a +32 product after the addition of peroxide in excess by mass spectrometry; and by the identification of sulfinic acid in C_P by partial sequencing of the peptide containing C_P after the treatment of the enzyme with hydrogen peroxide in excess and trypsin digestion (see Ref. [30] and Supplementary Fig. 1 and Tables IS and IIS).

Materials and methods

Chemicals

tert-Butylhydroperoxide (*t*-BuOOH), cumene hydroperoxide (cumeneOOH), 3-chloroperoxybenzoic acid (3-CPBA), sodium bicarbonate ($NaHCO_3$), 5,5′-dithiobis-(2-nitrobenzoate) (DTNB), soybean lipoxidase (LOX) type V, DTT, butylated hydroxytoluene (BHT), ferrous ammonium sulfate ($Fe(NH_4)_2(SO_4)_2$), and diethylenetriaminepentaacetic acid (DTPA) were purchased from Sigma–Aldrich. H_2O_2 was from Mallinckrodt Chemicals. 5*Z*,8*Z*,11*Z*,14*Z*-Eicosatetraenoic acid (arachidonic acid), (±)15-hydroxy-5*Z*,8*Z*,11*Z*,13*E*-eicosatetraenoic acid (15-HETE), 15*S*-hydroperoxy-5*Z*,8*Z*,11*Z*,13*E*-eicosatetraenoic acid (15-HpETE), 12*S*-hydroxy-5*Z*,8*Z*,10*E*,14*Z*-eicosatetraenoic-5,6,8,9,11,12,14,15-d8 acid (12-HETE-d8), and 9*Z*,12*Z*,15*Z*-octadecatrienoic acid (α-linolenic acid) were obtained from Cayman Chemicals. 3′,3″-Bis[bis(carboxymethyl)aminomethyl]cresolsulfonphthalein tetrasodium salt (xylenol orange) was from Applichem. Peroximonocarbonate (HCO_4^-) was obtained by the slow equilibrium reaction between H_2O_2 and bicarbonate as follows: $H_2O_2 + HCO_3^- \leftrightarrow HCO_4^- + H_2O$, $k_{on} = 3.1\times10^{-3}\ M^{-1}\ s^{-1}$, $k_{off} = 9.9\times10^{-3}\ s^{-1}$, $K_{eq} = 0.31\ M^{-1}$[35].

Both reactants were mixed and allow to equilibrate for 10–15 min so as to ensure equilibrium to be reached under the experimental conditions employed ($t_{1/2}$ = 1–1.1 min at 500 μM H_2O_2 and 50–150 mM HCO_3^-, pH 7.4, and 25 °C). HCO_4^- concentrations were calculated from K_{eq} and the reactant concentrations.

Linolenic acid peroxidation was produced by incubating α-linolenic acid (0.32 mM) with soybean LOX type V (9.5 nM) in 100 mM borate buffer plus 0.2% deoxycholate, pH 9 and 25 °C for 10 min. Reaction was stopped by adding, for lipid extraction purposes, a mixture of hexane/isopropanol/acetic acid (30/20/2, v/v/v) and lipids were extracted as reported [36]. Solvent was evaporated and lipids were resuspended into methanol and stored at −80 °C until used. Hydroperoxide concentrations before and after linolenic acid treatment with LOX were measured using the FOX assay (see below), with 15-HpETE as standard to obtain a calibration curve. Concentrations of fatty acid hydroperoxides were measured in parallel at 234 nm ($\varepsilon_{234} = 28{,}000\ M^{-1}\ cm^{-1}$[37]) with similar results.

Unless otherwise indicated, experiments were performed in 100 mM sodium phosphate buffer containing 0.1 mM DTPA, pH 7.4, and 25 °C.

Protein expression and purification

Wild-type *Mt*AhpE (TB database gene name Rv2238c) and a mutated form of the enzyme lacking the peroxidatic cysteine (C45S *Mt*AhpE) were expressed in *Escherichia coli* BL21(DE3) (expression vector pDEST17) as recombinant His-tagged proteins and purified as previously described [30].

Protein and thiol quantitation

*Mt*AhpE concentration was measured at 280 nm ($\varepsilon_{280} = 23{,}959\ M^{-1}\ cm^{-1}$ for both the wild-type and the mutant forms of the enzyme [30]). Protein thiol content was measured by Ellman's assay ($\varepsilon_{412} = 14{,}150\ M^{-1}\ cm^{-1}$) [38]. Recently purified *Mt*AhpE typically contained 0.9 thiol/protein and thiol content decreased with storage (under argon atmosphere, at −80 °C).

Protein thiol reduction and alkylation

*Mt*AhpE was reduced immediately before use by incubation with 1 mM DTT for 30 min at 4 °C. Excess reductant was removed by gel filtration using a HiTrap column (Amersham Bioscience) and UV–Vis detection at 280 nm. To avoid protein reoxidation, the elution buffer (100 mM sodium phosphate, pH 7.4, 0.1 mM DTPA) was extensively

degassed before use and samples were collected manually in rubber-capped tubes and maintained under argon atmosphere. In some cases, *Mt*AhpE C_P in reduced enzyme was alkylated by treatment with excess *N*-ethylmaleimide (NEM; 10 mM for 30 min) and excess NEM was removed by gel filtration as previously reported [30]. Residual thiol after alkylation was measured as above and was typically <10% of initial thiol content.

Changes in MtAhpE intrinsic fluorescence intensity

Emission spectra of reduced *Mt*AhpE before and after addition of various oxidizing substrates were recorded in an Aminco Bowman Series 2 luminescence spectrophotometer ($\lambda_{ex} = 295$ nm).

Kinetics of MtAhpE oxidation and overoxidation studies using a direct fluorimetric approach

The rate constants of *Mt*AhpE oxidation by various peroxides were determined by taking advantage of the decrease in the protein intrinsic fluorescence intensity upon oxidation as previously described [30]. Reduced *Mt*AhpE was rapidly mixed with the selected peroxide in excess in an Applied Photophysics SX-20 stopped-flow spectrofluorimeter (mixing time of ≤1.2 ms); the reaction was followed by total fluorescence intensity decrease ($\lambda_{ex} = 295$ nm) upon oxidation. Observed rate constants were determined by fitting stopped-flow data to single exponential functions. Second-order rate constants for the reaction between prereduced enzyme and the various peroxides at pH 7.4 were calculated from the slope of the plot of k_{obs} versus oxidant concentration. For the determination of the rate constant of *Mt*AhpE overoxidation by the various peroxides, we took advantage of the increase in the enzyme intrinsic fluorescence intensity that occurred upon treatment with a large excess of oxidant as previously reported [30]. In the case of *t*-BuOOH and cumeneOOH, enzyme overoxidation was followed using an Aminco Bowman Series 2 luminescence spectrofluorimeter ($\lambda_{ex} = 295$ nm; λ_{em} 335 nm), whereas for those peroxides that caused a faster overoxidation of the enzyme, reactions were followed by total fluorescence intensity increase using a stopped-flow spectrofluorimeter ($\lambda_{ex} = 295$ nm). In all cases, large excess peroxide concentrations with respect to enzyme were used; experimental curves were fitted to exponentials to obtain observed rate constants of reactions, which were plotted versus peroxide concentrations to determine the second-order rate constants for the reactions at pH 7.4. The real, pH-independent, rate constants ($k_{pH\ ind}$) were calculated from the rate constant measured at pH 7.4 ($k_{pH\ 7.4}$) and considering the proposed mechanism of reaction in which thiolate (in *Mt*AhpE oxidation) or sulfenate (in *Mt*AhpE overoxidation) and protonated peroxides are the reactive species [30,39],

$$k_{pH\ 7.4} = k_{pHind} \times \frac{K_{a_{MtAhpE-S(O)H}}}{K_{a_{MtAhpE-S(O)H}} + [H^+]} \times \frac{[H^+]}{K_{a_{ROOH}} + [H^+]} \quad (3)$$

where $K_{a\ MtAhpE\text{-}S(O)H}$ and $K_{a\ ROOH}$ are the acidic dissociation constants of *Mt*AhpE thiol (in oxidation reactions) or sulfenic acid (in overoxidation reactions) and the peroxide of interest, respectively.

Kinetics of MtAhpE reduction by DTT

We have previously demonstrated that oxidized enzyme was reduced by incubation with excess concentrations of DTT [30]. The kinetics of enzyme reduction was measured by following the increase in *Mt*AhpE fluorescence intensity that occurred when the enzyme was mixed with increasing DTT concentrations in excess. Experimental data were fit to single exponential curves. The rate constant of *Mt*AhpE reduction was determined from the slope of the plot of the observed rate constants of fluorescence change versus DTT concentration.

Catalytic and noncatalytic assay of peroxide reduction by MtAhpE

The catalytic reduction of various hydroperoxides by *Mt*AhpE using DTT as the reducing substrate was determined by following hydroperoxide concentrations using the FOX assay [40]. Briefly, 2 mM DTT and 2 μM *Mt*AhpE were incubated with the peroxide substrate (100 μM) in 50 mM sodium phosphate buffer plus 50 μM DTPA, pH 7.4, 25 °C. Aliquots (100 μl) were taken every 30 s and mixed with 900 μl of the FOX reagent (100 μM xylenol orange, 250 μM Fe^{2+}, 25 mM H_2SO_4, and 4 mM BHT in 90% (v/v) methanol) and further incubated for 30 min at room temperature before measurement at 560 nm. For measuring oxidizing substrate consumption by *Mt*AhpE under noncatalytic conditions, reduced enzyme (25 μM) was mixed with the hydroperoxide of interest (60 μM) and the concentrations of the latter at indicated times were also measured by the FOX assay. Extinction coefficients for H_2O_2, *t*-BuOOH, and cumeneOOH were determined as 53,050, 55,800, and 56,300 $M^{-1}\,cm^{-1}$, respectively, in close agreement with previously reported values [41]. For 15-HpETE the extinction coefficient was 78,500 $M^{-1}\,cm^{-1}$, which was higher than the value reported previously for another fatty acid hydroperoxide (linolenic acid hydroperoxide) [40]. Concentrations were confirmed by conjugated diene measurements at 234 nm ($\varepsilon_{234} = 28{,}000\ M^{-1}\,cm^{-1}$) [37].

Mass spectrometric analysis of 15-HpETE reduction

Reduced *Mt*AhpE (5 μM) or alkylated *Mt*AhpE (5 μM, 10% residual thiol) were exposed to equimolar concentrations of 15-HpETE; after 30 s, reaction products were extracted [36] and formation of 15-HETE was analyzed by liquid chromatography–tandem mass spectrometry. Before extraction, 10 ng of 12-HETE-d8 was added as an internal standard. Fatty acids were separated on a C_{18} ODS, 5-μm, 150×4.6-mm column (Waters Ltd.); the gradient used was 50–90% B over 40 min at 0.5 ml/min, with A being H_2O:ACN:acetic acid (75:25:0.1, v/v/v) and B being MeOH:ACN:acetic acid (60:40:0.1, v/v/v). Products were analyzed and quantified in the negative-ion mode on a Q-Trap 2000 (Applied Biosystems) using the following parent-to-daughter transitions of *m/z* in the multiple-reaction monitoring mode: *m/z* 319.2/219.1 (for 15-HETE) and *m/z* 327.2/184.1 (for 12-HETE-d8). Products were quantified using 12-HETE-d8 as an internal standard run in parallel under the same conditions.

Representation of MtAhpE under reduced state

Reduced *Mt*AhpE (PDB Accession No. 1XXU [29]) was represented using the Visual Molecular Dynamics program [42].

Results

Taking into account our previous work indicating that *Mt*AhpE C_P oxidation to sulfenic acid causes a decrease in enzyme intrinsic fluorescence intensity, and its overoxidation to sulfinic acid causes the fluorescence intensity to recover [30], we began an oxidizing substrate specificity study by analyzing the effects of various peroxides on the emission spectra of the enzyme. When reduced *Mt*AhpE (2 μM) was mixed with an equimolar concentration of *t*-BuOOH, a decrease in the enzyme intrinsic fluorescence intensity occurred during the first minutes of reaction that did not recover later (Fig. 1A). In addition, incubation of the enzyme with excess concentrations of *t*-BuOOH (100 μM) led to a rapid decrease followed by a slower increase in its fluorescence intensity (Fig. 1B). Similar results were obtained when using cumeneOOH as oxidant (not shown). The addition of increasing

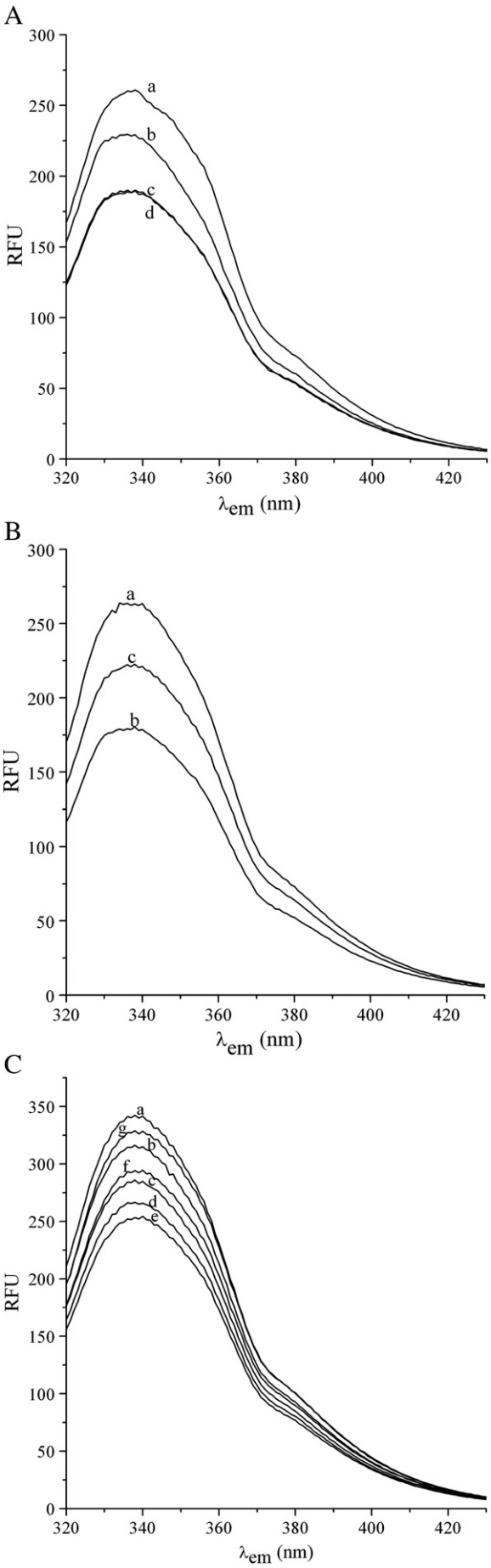

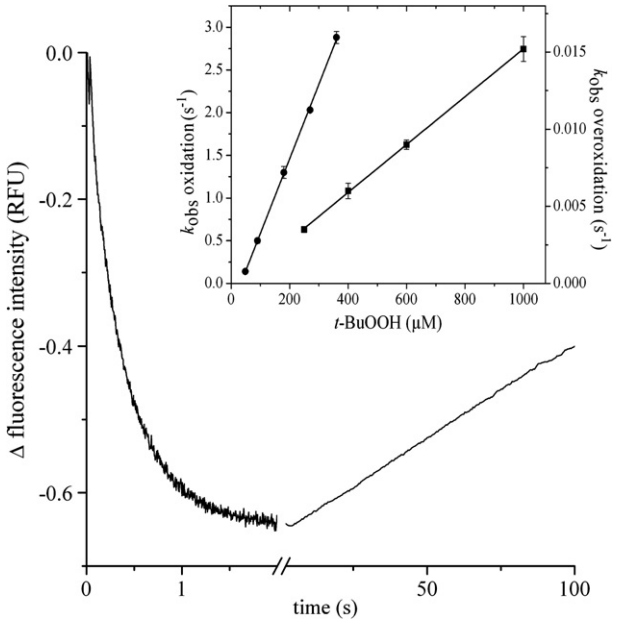

Fig. 2. Kinetics of *Mt*AhpE peroxidatic thiol oxidation and overoxidation by *t*-BuOOH. Reduced *Mt*AhpE (0.8 μM) was exposed to *t*-BuOOH (48 μM) in 100 mM sodium phosphate buffer plus 0.1 mM DTPA, pH 7.4 and 25 °C, and the time course of the total intrinsic fluorescence change ($\lambda_{ex} = 295$ nm) was recorded. The inset shows the effect of peroxide concentration on the observed rate constant of fluorescence change during the oxidation (circles) and overoxidation (squares) reactions.

substoichiometric concentrations of 15-HpETE (1.2–4.8 μM) to reduced *Mt*AhpE (5 μM) caused a rapid decrease in its intrinsic fluorescence intensity, consistent with C_P oxidation to sulfenic acid. Further additions of the oxidant caused *Mt*AhpE fluorescence intensity to increase, consistent with C_P overoxidation to sulfinic acid (Fig. 1C). The emission spectrum of reduced *Mt*AhpE was only minimally modified by similar concentrations of arachidonic acid, which most probably reflects the ~1% hydroperoxide contaminant in arachidonic stocks as determined by the FOX assay (not shown). Moreover, the addition of equimolar (Supplementary Fig. 1S) or excess (not shown) concentrations of 15-HpETE to C45S *Mt*AhpE (2 μM) caused no change in its intrinsic fluorescence intensity, indicating that the peroxidatic thiol was required for fluorescence changes to occur (Supplementary Fig. 1S). Similar results were previously described for H_2O_2- and peroxynitrite-dependent *Mt*AhpE fluorescence changes occurring upon enzyme oxidation and overoxidation [30].

Kinetics of MtAhpE oxidation and overoxidation by the organic hydroperoxides t-BuOOH and cumeneOOH

The time course of the reaction of reduced *Mt*AhpE (2 μM) with excess *t*-BuOOH was biphasic, showing a rapid decrease in its fluorescence intensity due to C_P oxidation, followed by a slower phase of fluorescence increase due to C_P overoxidation (Fig. 2). The rate constants of *t*-BuOOH-mediated oxidation and overoxidation of *Mt*AhpE increased with oxidant concentration and were determined as $(8.0 \pm 0.8) \times 10^3$ and $13 \pm 3\ M^{-1}\ s^{-1}$, respectively, at pH 7.4 and 25 °C

Fig. 1. Effects of *t*-BuOOH and 15-HpETE on intrinsic *Mt*AhpE emission spectra. (A) Emission spectra ($\lambda_{ex} = 295$ nm) of reduced *Mt*AhpE (2 μM) in 100 mM sodium phosphate buffer, 0.1 mM DTPA, pH 7.4, 25 °C, before (trace a) and 1 (trace b), 4 (trace c), and 6 min (trace d) after the addition of *t*-BuOOH (2 μM). (B) Same as (A) but before (trace a) and 1 (trace b) and 6 min (trace c) after the addition of *t*-BuOOH (100 μM). (C) Emission spectra of reduced *Mt*AhpE (5 μM) in the same buffer as in (A) before (a) and 1 min after the addition of increasing concentrations of 15-HpETE (traces b, 1.2 μM; c, 2.4 μM; d, 3.6 μM; e, 4.8 μM; f, 6.0 μM; and g, 7.2 μM).

Table 1
Kinetics of *Mycobacterium tuberculosis* AhpE oxidation and overoxidation by various peroxides.

ROOH	pK_a	p$K_{a\ ROH}$	$k_{ox\ pH\ 7.4}$ ($M^{-1}\ s^{-1}$)	$k_{ox\ pH\ ind}$ ($M^{-1}\ s^{-1}$)	$k_{overox\ pH\ 7.4}$ ($M^{-1}\ s^{-1}$)	$k_{overox\ pH\ ind}$ ($M^{-1}\ s^{-1}$)	Reference
H_2O_2	11.7	15.7	8.2×10^4	8.2×10^4	40	46	[30]
ONOOH	6.8	3.15	1.9×10^7	9.5×10^7	ND	ND	[30]
t-BuOOH	12.8	18	8.0×10^3	8.0×10^3	13	15	This work
CumeneOOH	12.6	14.5	4.0×10^4	4.0×10^4	65	76	This work
HCO_4^-	>9	10.3	1.1×10^7	1.1×10^7	2.1×10^3	2.5×10^3	This work
3-CPBA	7.57	3.82	2.4×10^7	3.9×10^7	2.0×10^5	3.8×10^5	This work
15-HpETE	>10[a]	>10[a]	1.8×10^8	1.8×10^8	3.9×10^5	4.5×10^5	This work
α-Linolenic acid hydroperoxides[b]	>10[a]	>10[a]	2.7×10^8	2.7×10^8	3.7×10^5	4.0×10^5	This work

pK_a indicates the pK_a value of the peroxide (ROOH) functional group. p$K_{a\ ROH}$ stands for leaving-group pK_a and indicates the pK_a value of the product formed upon peroxide reduction (ROH). k_{ox} and $k_{overox\ pH\ 7.4}$ are the rate constants of *Mt*AhpE oxidation to and overoxidation at pH 7.4 and 25 °C, respectively; k_{ox} and $k_{overox\ pH\ ind}$ are the pH-independent rate constants of *Mt*AhpE oxidation to and overoxidation at 25 °C, respectively. Reference refers to the kinetics values; references related to pK_a values are provided in the text.

[a] Although pK_a values for the hydroperoxide group in 15-HpETE or the alcohol group in 15-HETE have not been determined, they should be similar to those of other alkyl hydroperoxides and alcohols, respectively, and therefore can be safely assumed to be >10.

[b] Mixture of hydroperoxides formed from the LOX-catalyzed oxidation of α-linolenic acid.

(Fig. 2, inset). Similarly, the rate constants of *Mt*AhpE oxidation and overoxidation by cumeneOOH were determined as $(4.0\pm0.2)\times10^4$ and $65\pm7\ M^{-1}\ s^{-1}$ under the same experimental conditions (Supplementary Fig. 2S). According to Eq. (3)—considering reported pK_a values of *t*-BuOOH (12.8) and cumeneOOH (12.6) [43], as well as pK_a values of *Mt*AhpE peroxidatic thiol and sulfenic acid of 5.2 and 6.6, respectively [30]—real (pH-independent) rate constants were calculated as 8×10^3 and $4\times10^4\ M^{-1}\ s^{-1}$ for *t*-BuOOH- and cumeneOOH-mediated C_P oxidation, respectively, and 15 and $76\ M^{-1}\ s^{-1}$ for *t*-BuOOH- and cumeneOOH-mediated C_P overoxidation, respectively (Table 1). These pH-independent values were equal or very similar to those obtained at pH 7.4, because the mechanism of reaction involves the protonated peroxide species and the thiolate (for oxidation) or sulfenate (for overoxidation) forms of C_P in *Mt*AhpE, which are by far the predominant species at the indicated pH.

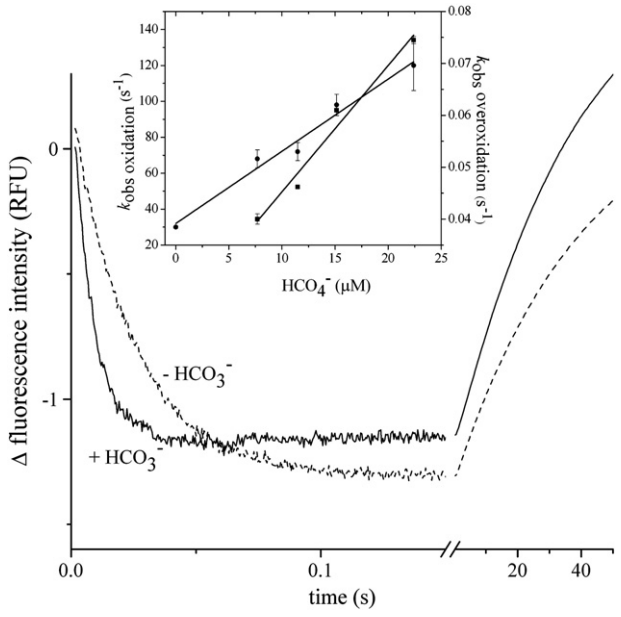

Fig. 3. Kinetics of *Mt*AhpE thiol oxidation and overoxidation by HCO_4^-. Reduced *Mt*AhpE (1 μM) was rapidly mixed with solutions of H_2O_2 (500 μM) without any further addition (dashed line, $-HCO_3^-$) or preequilibrated with 100 mM HCO_3^- to allow HCO_4^- formation (continuous line, $+HCO_3^-$), in sodium phosphate buffer plus 0.1 mM DTPA, pH 7.4 and 25 °C, and the rapid phase of fluorescence decrease corresponding to *Mt*AhpE oxidation followed by a slower phase of fluorescence increase due to overoxidation was measured using a stopped-flow spectrofluorimeter (λ_{ex} = 295 nm). The inset shows the effect of increasing HCO_4^- concentrations (calculated from the reported K_{eq} values, see Materials and methods) on the k_{obs} of *Mt*AhpE fluorescence change during the oxidation (circles) and overoxidation (squares) phases of the reaction.

Kinetics of MtAhpE oxidation and overoxidation by HCO_4^- and 3-chloroperoxybenzoic acid

When reduced *Mt*AhpE (1 μM) was rapidly mixed with increasing concentrations of preformed HCO_4^-, biphasic changes in fluorescence intensity, consistent with C_P oxidation followed by overoxidation, were observed (Fig. 3). Observed rate constants of each phase were slower for *Mt*AhpE treatment with H_2O_2 alone (in agreement with reported rate constant values of H_2O_2-mediated *Mt*AhpE oxidation ($(8.2\pm1.5)\times10^4\ M^{-1}\ s^{-1}$) and overoxidation ($40\pm3\ M^{-1}\ s^{-1}$) [30]) and were faster in the presence of increasing concentrations of HCO_4^-. The rate constants of *Mt*AhpE oxidation and overoxidation by HCO_4^- were determined as $(1.1\pm0.4)\times10^7$ and $(2.1\pm0.8)\times10^3\ M^{-1}\ s^{-1}$ at pH 7.4 and 25 °C (Fig. 3, inset). According to Eq. (3) and assuming a pK_a value for HCO_4^- dissociation >9 [44], and the above-mentioned pK_a values of the peroxidatic thiol and sulfenic acid at *Mt*AhpE [30], the pH-independent rate constants of HCO_4^--mediated *Mt*AhpE oxidation and overoxidation were calculated as 1.1×10^7 and $2.5\times10^3\ M^{-1}\ s^{-1}$ (Table 1). Similarly, the kinetics of the reaction of 3-chloroperoxybenzoic acid (a stable artificial peracid with a low leaving-group pK_a) with reduced *Mt*AhpE were determined as 2.4×10^7 and $(2.0\pm0.2)\times10^5\ M^{-1}\ s^{-1}$ at pH 7.4 and 25 °C for enzyme oxidation and overoxidation, respectively (Supplementary Fig. 3S). According to Eq. (3) and considering the pK_a values of 3-CPBA (7.5 [45]), *Mt*AhpE thiol, and sulfenic acid, the pH-independent rate constants of 3-CPBA-mediated *Mt*AhpE oxidation and overoxidation were calculated as 3.9×10^7 and $3.8\times10^5\ M^{-1}\ s^{-1}$, respectively (Table 1).

Kinetics of MtAhpE oxidation and overoxidation by 15-HpETE

When reduced *Mt*AhpE (2 μM) was rapidly mixed with excess 15-HpETE, a single phase of increase in enzyme intrinsic fluorescence was observed (not shown). Only at very low (<3 μM) 15-HpETE concentrations was the fast decrease in fluorescence intensity due to enzyme oxidation apparent in our stopped-flow apparatus (mixing time <2 ms), indicating a very fast reaction between the enzyme and this oxidant (Fig. 4A). Arachidonic acid by itself did not cause any change in *Mt*AhpE fluorescence intensity during the same time scale (Fig. 4A). Methanol, used as vehicle in stock arachidonic acid and 15-HpETE solution, had no effect on the enzyme fluorescence spectra at the concentrations used (not shown). The rate constants of 15-HpETE-dependent *Mt*AhpE oxidation and overoxidation were $(1.8\pm0.3)\times10^8$ and $(3.9\pm0.5)\times10^5\ M^{-1}\ s^{-1}$, respectively, at pH 7.4 and 25 °C (Fig. 4B). Because the hydroperoxide functional group of 15-HpETE is fully protonated at pH <9, pH-independent rate constants were calculated according to Eq. (3) as 1.8×10^8 and $4.5\times10^5\ M^{-1}\ s^{-1}$ for *Mt*AhpE oxidation and overoxidation, respectively (Table 1).

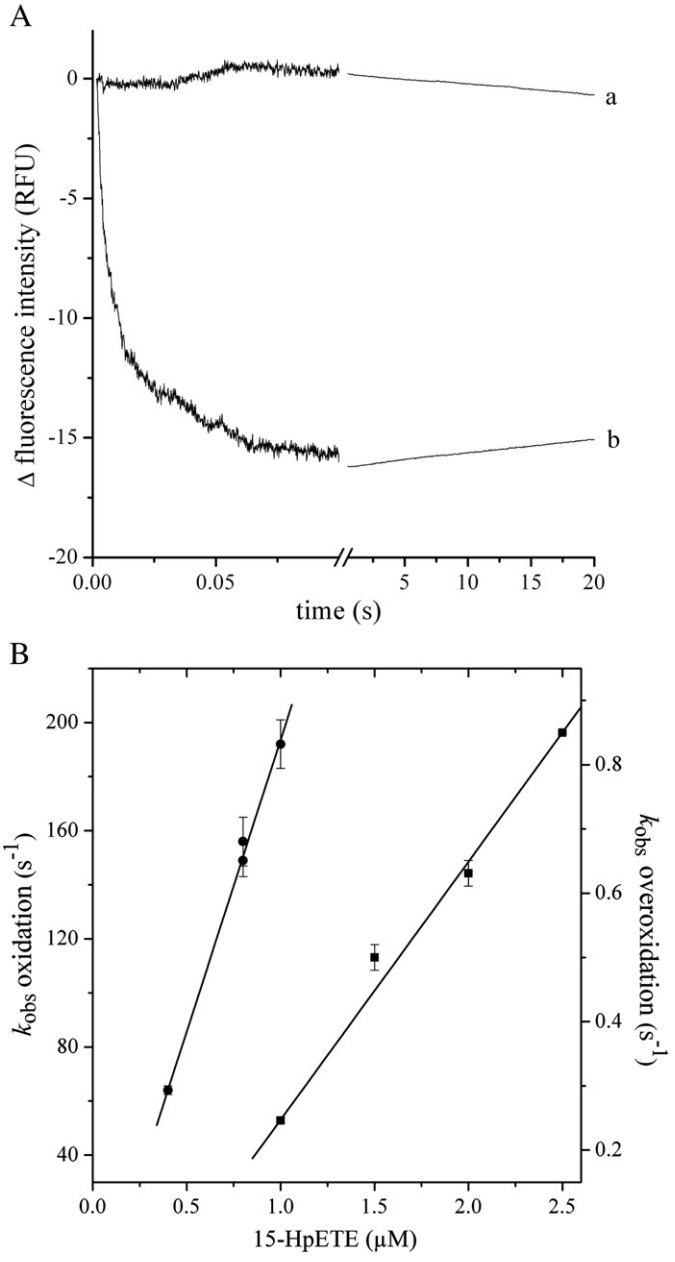

Fig. 4. Kinetics of *Mt*AhpE thiol oxidation and overoxidation by 15-HpETE. (A) Reduced *Mt*AhpE (2 μM) was exposed to arachidonic acid (2 μM; trace a) or 15-HpETE (2 μM; trace b) in 100 mM sodium phosphate buffer plus 0.1 mM DTPA, pH 7.4 and 25 °C, and the time course of the total intrinsic fluorescence change ($\lambda_{ex} = 295$ nm) was recorded. (B) Reduced *Mt*AhpE (0.2 μM) was exposed to excess 15-HpETE in the same buffer as in (A), and the rapid first phase of fluorescence intensity decreased (due to enzyme oxidation, circles), whereas the slower phase of fluorescence intensity increased (due to enzyme overoxidation, squares), fitted to exponential curves. The observed rate constants of oxidation and overoxidation were plotted versus 15-HpETE concentration to determine the rate constants of both processes.

To test whether the rapid 15-HpETE-mediated *Mt*AhpE oxidation and overoxidation observed were specific or also occurred for other long-chain fatty acid hydroperoxides, we tested the effects of α-linolenic acid-derived hydroperoxides formed upon LOX-mediated α-linolenic acid oxidation on the enzyme. The addition of excess α-linolenic acid hydroperoxides to reduced *Mt*AhpE caused biphasic fluorescence changes consistent with enzyme oxidation and overoxidation (Supplementary Fig. 4S). Neither the addition of α-linolenic acid to reduced enzyme nor the addition of LOX-treated α-linolenic acid to alkylated enzyme caused any change in *Mt*AhpE intrinsic fluorescence intensity. The rate constants of α-linolenic acid-derived hydroperoxide-mediated *Mt*AhpE oxidation and overoxidation were $(2.7 \pm 1) \times 10^8$ and $3.7 \times 10^5\ M^{-1}\ s^{-1}$, respectively, at pH 7.4 and 25 °C, quite similar to the rate constant for pure 15-HpETE-mediated oxidation (Supplementary Fig. 4S).

Catalytic activity of MtAhpE using various oxidizing substrates

We next evaluated the ability of *Mt*AhpE to catalyze various hydroperoxide reductions, using DTT as reducing substrate. *Mt*AhpE

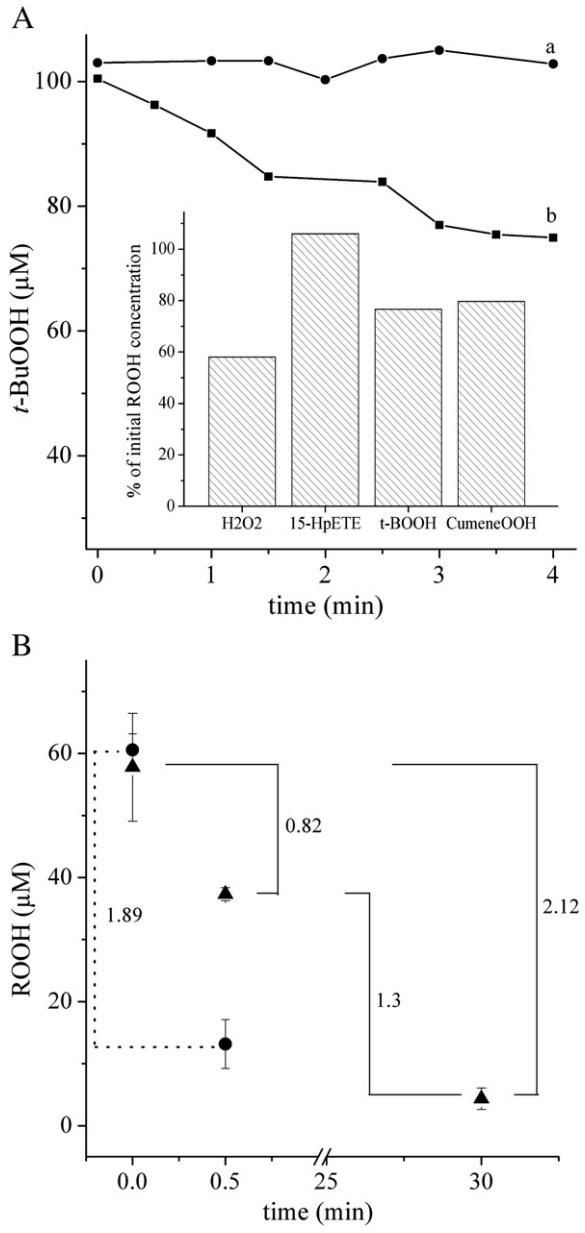

Fig. 5. Reduction of hydroperoxides by reduced *Mt*AhpE. (A) Catalytic activity of *Mt*AhpE using various hydroperoxides as oxidizing substrates. Time course of *t*-BuOOH (100 μM) consumption by DTT (2 mM) in the absence (line a, black circles) or in the presence (line b, black squares) of *Mt*AhpE (2 μM), in 50 mM sodium phosphate buffer, pH 7.4 and 25 °C. The inset shows percentages of initial hydroperoxide concentrations that are left after 3 min incubation with DTT (2 mM) in the presence of *Mt*AhpE (2 μM). (B) Oxidation yields of H_2O_2- and 15-HpETE-mediated *Mt*AhpE oxidation. Hydroperoxide concentrations before and 30 s or 30 min after the addition of reduced *Mt*AhpE (25 μM) in 50 mM sodium phosphate buffer, pH 7.4. Black cycles, 15-HpETE; black triangles, H_2O_2. Numbers next to continuous lines (for H_2O_2) or dotted lines (for 15-HpETE) indicate the stoichiometries of peroxide consumption by *Mt*AhpE at the indicated times of incubation.

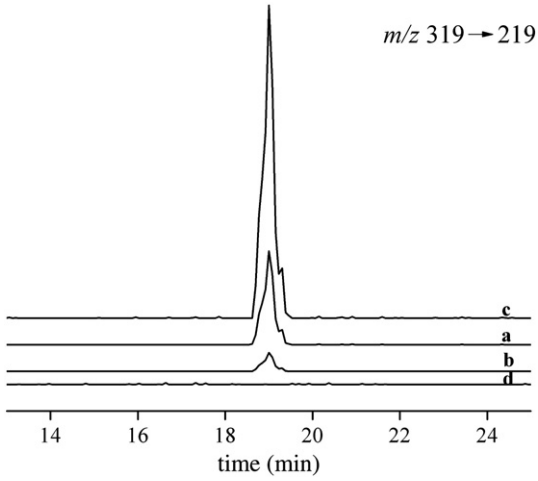

Fig. 6. 15-HETE formation from 15-HpETE reduction by *Mt*AhpE. Reduced (line a) or alkylated *Mt*AhpE (5 μM) (line b) was mixed with 15-HpETE (5 μM) in sodium phosphate buffer plus 0.1 mM DTPA, pH 7.4, and after 30 s of reaction 15-HETE formation was measured by mass spectrometry. Line c shows the peak corresponding to a standard solution of 15-HETE (3 μM), and line d is 3 μM 15-HpETE without any further addition.

(2 μM) catalyzed H_2O_2, *t*-BuOOH, and cumeneOOH reduction by DTT (2 mM) (Fig. 5A). However, no 15-HpETE (100 μM) catalytic consumption by DTT (2 mM) was observed (Fig. 5 inset). Because 15-HpETE-mediated overoxidation is ~10^4 times faster than that produced by *t*-BuOOH or cumeneOOH, we considered the possibility that the enzyme could be inactivated by excess 15-HpETE reaction with the sulfenate form of the enzyme prior reduction by DTT. Therefore, we measured the rate constant of DTT-mediated *Mt*AhpE reduction, which was 90 M^{-1} s^{-1} at pH 7.4 and 25 °C (Supplementary Fig. 5S). Thus, under the conditions of the assay ([DTT] 2 mM, [peroxide] 100 μM), DTT-mediated reduction would be able to compete with enzyme overoxidation by H_2O_2, *t*-BuOOH, and cumeneOOH but would be too slow to compete with enzyme overoxidation by 15-HpETE.[2]

Noncatalytic reduction of 15-HpETE to 15-HETE by MtAhpE

The addition of 15-HpETE (40 μM) to reduced *Mt*AhpE (52 μM) caused a stoichiometric oxidation of *Mt*AhpE thiol groups, as measured by the DTNB assay. As expected, arachidonic acid (40 μM) did not cause any thiol oxidation on reduced *Mt*AhpE (data not shown). Incubation of 15-HpETE (60 μM) with reduced *Mt*AhpE (25 μM) in sodium phosphate buffer, pH 7.4 and 25 °C, caused the reduction of 50 μM 15-HpETE in 30 s (Fig. 5B). This consumption is in agreement with a rapid C_P oxidation and overoxidation, which according to the kinetics reported above, should be completed in the indicated time ($t_{1/2}$ oxidation at 60 μM 15-HPETE <0.1 ms; $t_{1/2}$ overoxidation at remaining 35 μM 15-HpETE 0.05 s). Moreover, H_2O_2 (60 μM) reduction by *Mt*AhpE (25 μM) under the same conditions showed a 1:1 stoichiometry in 30 s and a 2:1 stoichiometry in 30 min (Fig. 5B). This is consistent with the slower rate constants of *Mt*AhpE oxidation and overoxidation by H_2O_2 compared with 15-HpETE [30] ($t_{1/2}$ oxidation at 60 μM H_2O_2 0.14 s, $t_{1/2}$ overoxidation at remaining 35 μM H_2O_2 8 min, calculated according to the rate constant reported in [30]).

Incubation of 15-HpETE (5 μM) with reduced *Mt*AhpE (5 μM) for 30 s in 100 mM sodium phosphate buffer plus 0.1 mM DTPA, pH 7.4, caused the formation of 15-HETE (Fig. 6, line a), which coeluted with the 15-HETE standard (Fig. 6, line c) and displayed the characteristic mass transition *m/z* 319/219. Quantitative determinations using 12-HETE-d8 as internal standard showed that 5 μM *Mt*AhpE caused the formation of 4.86 ± 0.23 μM 15-HETE. The amount of 15-HETE formed from 15-HpETE (5 μM) incubation with alkylated *Mt*AhpE (5 μM, 0.5 μM remaining thiols) was much lower (line b), 1.31 ± 0.64 μM, consistent with the small fraction of remaining thiols still available in the enzyme after treatment with NEM, which through oxidation and overoxidation reactions could lead to up to two 15-HETE/thiol formation. 15-HpETE (5 μM) without any further addition showed no contaminating 15-HETE (line d).

Discussion

In a previous work, we reported that peroxynitrite reduction by the C_P in *Mt*AhpE was approximately 3 orders of magnitude faster than H_2O_2 reduction [30]. However, the molecular bases for those differential reactivities, as well as the possibility of other potential biologically relevant oxidizing substrates for the enzyme, were not investigated. Herein, we performed a comprehensive study on *Mt*AhpE oxidizing substrate specificity as well as on its oxidative inactivation by various peroxides, which could contribute to our understanding of the antioxidant systems that might play a role in *M. tuberculosis* success during host infection. Moreover, some of the results obtained could help to rationalize the molecular mechanisms of peroxide reduction by Prxs in general.

Peroxide reduction by thiolates is an SN2 or direct displacement reaction. The reaction takes place via the nucleophilic attack of the thiolate on one of the peroxide oxygens; a transition state is reached in which the negative charge of the attacking group is distributed among the two oxygen atoms and the sulfur. To complete the reaction the peroxide bond should break to release the leaving group. In the case of the low-molecular-weight thiol glutathione and the single free thiol of bovine serum albumin, reaction rates of thiolate oxidation are higher for peroxides with the lower leaving-group pK_a (i.e., the pK_a of the product formed upon peroxide reduction) [35]. For most peroxides tested, *Mt*AhpE peroxidatic thiol oxidation was also faster for those peroxides with the lower leaving-group pK_a (Fig. 7, Table 1). This could explain the ~10^3 times faster *Mt*AhpE-dependent peroxynitrite reduction compared to H_2O_2 reduction that we previously reported [30] and can be easily observed as a negative correlation between intrinsic thiolate reactivities ($k_{2\ pH\ ind}$) and leaving-group pK_a value shown as a Brønsted plot in Fig. 7. From the slope of this plot, a nucleophilic constant of the leaving group (β_{Lg}) of −0.27 was obtained, which is similar to that reported for peroxide-mediated GSH oxidation ($\beta_{Lg} = -0.32$, calculated from data reported in [35]), indicating that nucleophilic characteristics of leaving groups are important for defining the rate constant of the reactions. Of note, despite the similar trend in reactivities with leaving-group pK_a, rate constants of peroxide-mediated peroxidatic thiol oxidation in *Mt*AhpE are ~10^3–10^4 times faster than those of low-molecular-weight thiol oxidation, as has already been described for other Prxs.[3] The protein factors responsible for such extraordinary increase in catalytic cysteine oxidation rates in peroxiredoxins are still a matter of speculation, although transition state stabilization is most probably involved [47].

[2] Rate constant times reactant concentration for DTT-mediated *Mt*AhpE reduction and peroxide-mediated *Mt*AhpE overoxidation should be compared. Hence, DTT-mediated enzyme reduction at pH 7.4 (90 M^{-1} s^{-1} × 2 × 10^{-3} M = 0.180 s^{-1}) would be competed by enzyme overoxidation by 15-HpETE (3.9 × 10^5 M^{-1} s^{-1} × 100 × 10^{-6} M = 39 s^{-1}) but not by overoxidation by H_2O_2 (40 M^{-1} s^{-1} × 100 × 10^{-6} M = 4 × 10^{-3} s^{-1}), *t*-BuOOH (13 M^{-1} s^{-1} × 100 × 10^{-6} M = 1.3 × 10^{-3} s^{-1}), or cumeneOOH (65 M^{-1} s^{-1} × 100 × 10^{-6} M = 6.5 × 10^{-3} s^{-1}) under the experimental conditions of the assays.

[3] In the case of some Prxs, reaction rates can be even >>10^4 faster compared to free cysteine oxidation, as for H_2O_2-mediated red blood cell Prx2 oxidation ($k_{pH\ ind}$ = 1 × 10^8 M^{-1} s^{-1} [32] versus 18 M^{-1} s^{-1} for cysteine oxidation [46]).

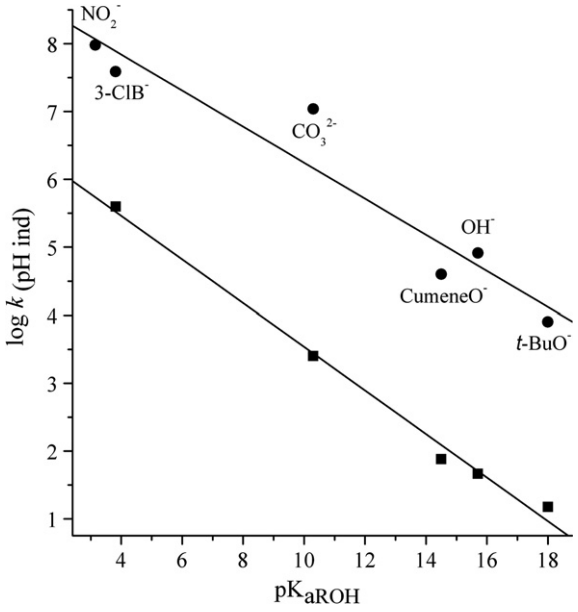

Fig. 7. Brønsted plot relationship for the reactivities of various peroxides with reduced or oxidized *Mt*AhpE. pH-independent rate constants for various peroxide-mediated oxidations (circles) and overoxidations (squares) of *Mt*AhpE were calculated from the experimentally determined rate constants at pH 7.4 using Eq. (3). Logarithms of pH-independent rate constants were plotted versus the pK_a values for the conjugated acids of the alkoxides formed as products from peroxide reductions (leaving-group pK_a). Peroxides utilized were peroxynitrite (leaving group nitrite anion, NO_2^-), 3-CPBA (leaving group 3-chlorobenzoate, 3-ClB$^-$), HCO_4^- (leaving group carbonate anion, CO_3^{2-}), cumeneOOH (leaving group cumene alkoxide, cumeneO$^-$), H_2O_2 (leaving group hydroxyl anion, OH$^-$), *t*-BuOOH (leaving group *tert*-butylalkoxide, *t*-BuO$^-$). Rate constants and pK_a values are shown in Table 1.

Based on the pH profile for H_2O_2-mediated *Mt*AhpE overoxidation, we postulated a mechanism of reaction in which sulfenate (RSO$^-$) and protonated peroxide were the reactive species (Eq. (2)) [30]. However, the pH profile could in fact also be explained by a mechanism of reaction involving sulfenic acid (RSOH) and HOO$^-$, though a much faster pH-independent rate constant would be required to explain the results, so as to compensate for the small fraction of sulfenic acid (pK_a = 6.6 [30]) and, more importantly, HOO$^-$ (pK_a H_2O_2 = 11.7 [48]) that would be present at the pH range explored (5<pH<8). Herein, we also found an inverse correlation between the pH-independent rate constant of peroxide-dependent *Mt*AhpE C_P overoxidation to sulfinic acid and the leaving-group pK_a, indicating that both C_P oxidation and overoxidation occur by similar mechanisms of reaction. This is consistent with sulfenate (RSO$^-$) (or its tautomeric sulfoxide [49]) being the reactive species, as originally proposed [30].

In the case of 15-HpETE, the rate constants of *Mt*AhpE oxidation and overoxidation (Fig. 4, Table 1) were much higher than expected from the Brønsted relationship shown in Fig. 7. Although the pK_a of 15-HETE, the product formed from *Mt*AhpE-dependent 15-HpETE reduction (Fig. 6), has not been reported, it should be in the range of other aliphatic alcohols and similar to those of H_2O_2, *t*-BuOOH, and cumeneOOH (i.e., >10). The reaction rates determined in Fig. 4B (1.8×10^8 and 3.9×10^5 M^{-1} s^{-1} for *Mt*AhpE oxidation and overoxidation, respectively) were surprisingly fast. Rate constants were confirmed by other approaches: a 2:1 15-HpETE reduction per *Mt*AhpE thiol group upon 30 s incubation time indicated that the enzyme was oxidized and overoxidized much faster than by H_2O_2 treatment, which required 30 min for the same stoichiometry to be achieved (Fig. 5B). Moreover, the fast oxidative inactivation produced by *Mt*AhpE sulfenate reaction with 15-HpETE compared with DTT-dependent reduction (k = 90 M^{-1} s^{-1}, Supplementary Fig. 5S) explains that whereas the enzyme consumed rapidly 15-HpETE under noncatalytic conditions (Fig. 5B), no catalytic activity could be observed when using DTT as reducing substrate, which cannot compete with the oxidative inactivation (Fig. 5A) (k = 90 M^{-1} s^{-1}, Supplementary Fig. 5S). Thus, *Mt*AhpE reduced 15-HpETE (Fig. 4) and α-linolenic acid-derived hydroperoxides (Supplementary Fig. 4S) with rate constants that were even faster than those of the mammalian selenium-containing glutathione peroxidase 4, the enzyme with the greatest reactivity toward fatty acid hydroperoxides that had been identified so far [50]. The rate constant for C_P oxidation was as fast as human red blood cell Prx2 oxidation by H_2O_2[32]. In the case of *Mt*AhpE overoxidation to sulfinic acid, similarly rapid reactions have been reported for linolenic acid hydroperoxide-mediated OhrR overoxidation to sulfinic acid, which occurs with a rate constant of 2×10^5 M^{-1} s^{-1}[51]. The enzyme is also rapidly inactivated by these hydroperoxides, in a way that precludes the measurement of enzymatic activity using artificial DTT as reducing substrate. The identification of potential natural reducing substrates that could support *Mt*AhpE catalytic activity before oxidative inactivation occurs would be the subject of future work.

Deviation from the expected Brønsted plot correlations with leaving-group pK_a is frequent in Prx-mediated peroxide reductions. In the case of human Prx5, oxidation was much faster with peroxynitrite than with H_2O_2, consistent with the former having a lower leaving-group pK_a[31]. However, when *t*-BuOOH- and

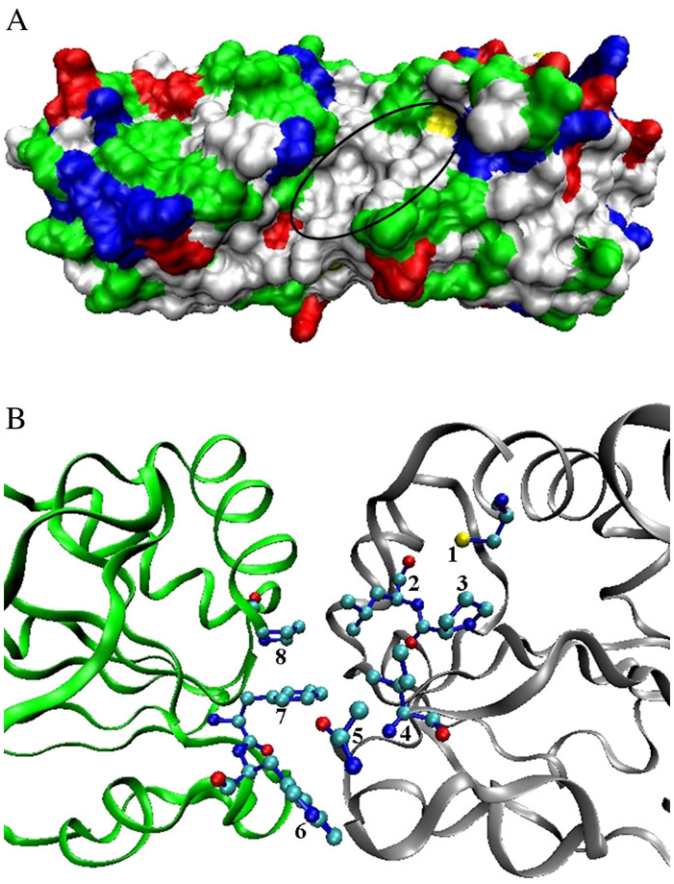

Fig. 8. Representations of reduced *Mt*AhpE (PDB Accession No. 1XXU [27]) show a surface-exposed hydrophobic groove. (A) The molecular surface of reduced *Mt*AhpE is colored according to residue type (blue, basic; red, acidic; green, polar; white, nonpolar). Cysteine 45 (C_P) is shown in yellow. The black oval indicates a hydrophobic groove close to C_P. (B) C_P of subunit A (Cys 45; 1) and non-polar amino acids that form the hydrophobic groove shown in (A): Ile 113 (2), Pro 38 (3), Leu 39 (4), and Ala 111 (5) from subunit A (silver ribbons); Trp 95 (6), Phe 94 (7), and Pro 73 (8) from subunit B (green ribbons) of the homodimeric enzyme. In those residues, atoms are colored according to their type: red, oxygen; blue, nitrogen; yellow, sulfur.

cumeneOOH-mediated oxidations were analyzed, they greatly deviated above the reactivity trend. The crystal structure of reduced Prx5 presents a benzoate ion in close association with the active site [52], with one side of the active-site pocket containing several hydrophobic residues whose side chains are located in the neighborhood of the benzoate aromatic ring. Similar interactions could contribute to the fast reactivity of this enzyme with aliphatic or aromatic hydrophobic peroxides. In the case of all typical two-cysteine Prxs whose reactivity toward H_2O_2 and peroxynitrite has been determined so far, the former reacts equally or even faster than the latter oxidant, with the molecular reasons for this remaining unknown [32–34,53,54], and data regarding the kinetics of fatty acid hydroperoxide-mediated oxidation or overoxidation are lacking. Concerning *Mt*AhpE, a noncovalent homodimeric enzyme, the reported structure of the reduced enzyme reveals a surface hydrophobic groove, which could serve as an anchoring site for fatty acid hydroperoxide binding (Fig. 8A). The groove is formed by nonpolar amino acids from the two subunits of the enzyme, namely Ile 113, Leu 39, Pro 38, and Ala 111 from subunit A and Phe 94, Trp 95, and Pro 73 from subunit B (Fig. 8B), whose hydrophobic interactions with these kinds of substrates could be the basis of their deviation from the general Brønsted correlation observed for other substrates (Fig. 7).

*Mt*AhpE belongs to a new family of Prxs, comprising bacterial and achaean AhpE and AhpE-like enzymes. Functional data for any member of the group other than *Mt*AhpE are lacking. Our data constitute a first step toward the characterization of this novel group of Prxs, for which we postulate a role in lipid-derived hydroperoxide reduction, in addition to the peroxynitrite reductase activity reported in our previous work [30]. In this regard, it is interesting that AhpE was identified in the membrane fraction of *M. tuberculosis* using a proteomics approach [25]. Free arachidonic acid is toxic to *M. tuberculosis* and this toxicity was found to be synergistic with that produced by reactive nitrogen species [55]. The mechanism behind the synergism is not clear in these bacteria, but the fact that free fatty acid-dependent toxicity to *Helicobacter pylori* increases in peroxidase-deficient strains indicates that fatty acid hydroperoxides are probably involved in the process leading to cell death [12]. Antioxidant systems such as the one described herein are of particular interest for understanding the mechanisms that contribute to the success of *M. tuberculosis* in infection processes and identifying novel potential therapeutic targets for tuberculosis treatment.

Acknowledgments

The authors thank ANII for financial support (FCE_516) to A.T. A.R. and M.H. were partially supported by fellowships from ANII. We also thank Marcelo Martí and Darío Estrín (Departamento de Química Inorgánica, Analítica y Química Física/INQUIMAE-CONICET, Facultad de Ciencias Exactas y Naturales, Universidad de Buenos Aires, Argentina) for helpful discussion. R.R. is a Howard Hughes Medical Institute Research Scholar.

Appendix A. Supplementary data

Supplementary data to this article can be found online at doi:10.1016/j.freeradbiomed.2011.04.023.

References

[1] Andersen, P. Vaccine strategies against latent tuberculosis infection. *Trends Microbiol.* **15:**7–13; 2007.
[2] Brandt, L.; Feino Cunha, J.; Weinreich Olsen, A.; Chilima, B.; Hirsch, P.; Appelberg, R.; Andersen, P. Failure of the Mycobacterium bovis BCG vaccine: some species of environmental mycobacteria block multiplication of BCG and induction of protective immunity to tuberculosis. *Infect. Immun.* **70:**672–678; 2002.
[3] Harries, A. D.; Zachariah, R.; Corbett, E. L.; Lawn, S. D.; Santos-Filho, E. T.; Chimzizi, R.; Harrington, M.; Maher, D.; Williams, B. G.; De Cock, K. M. The HIV-associated tuberculosis epidemic—when will we act? *Lancet* **375:**1906–1919; 2010.
[4] Kaye, K.; Frieden, T. R. Tuberculosis control: the relevance of classic principles in an era of acquired immunodeficiency syndrome and multidrug resistance. *Epidemiol. Rev.* **18:**52–63; 1996.
[5] Meena, L. S.; Rajni Survival mechanisms of pathogenic Mycobacterium tuberculosis H37Rv. *FEBS J.* **277:**2416–2427; 2010.
[6] Yoshida, A.; Inagawa, H.; Kohchi, C.; Nishizawa, T.; Soma, G. The role of toll-like receptor 2 in survival strategies of Mycobacterium tuberculosis in macrophage phagosomes. *Anticancer Res.* **29:**907–910; 2009.
[7] Rajavelu, P.; Das, S. D. A correlation between phagocytosis and apoptosis in THP-1 cells infected with prevalent strains of Mycobacterium tuberculosis. *Microbiol. Immunol.* **51:**201–210; 2007.
[8] Fang, F. C. Antimicrobial reactive oxygen and nitrogen species: concepts and controversies. *Nat. Rev. Microbiol.* **2:**820–832; 2004.
[9] Nathan, C.; Shiloh, M. U. Reactive oxygen and nitrogen intermediates in the relationship between mammalian hosts and microbial pathogens. *Proc. Natl Acad. Sci. U. S. A.* **97:**8841–8848; 2000.
[10] Alvarez, M. N.; Peluffo, G.; Piacenza, L.; Radi, R. Intraphagosomal peroxynitrite as a macrophage-derived cytotoxin against internalized Trypanosoma cruzi: consequences for oxidative killing and role of microbial peroxiredoxins in infectivity. *J. Biol. Chem.* **286:**6627–6640; 2011.
[11] Radi, R.; Beckman, J. S.; Bush, K. M.; Freeman, B. A. Peroxynitrite-induced membrane lipid peroxidation: the cytotoxic potential of superoxide and nitric oxide. *Arch. Biochem. Biophys.* **288:**481–487; 1991.
[12] Porter, N. A.; Caldwell, S. E.; Mills, K. A. Mechanisms of free radical oxidation of unsaturated lipids. *Lipids* **30:**277–290; 1995.
[13] Lewis, J. G.; Hamilton, T.; Adams, D. O. The effect of macrophage development on the release of reactive oxygen intermediates and lipid oxidation products, and their ability to induce oxidative DNA damage in mammalian cells. *Carcinogenesis* **7:**813–818; 1986.
[14] Bonney, R. J.; Opas, E. E.; Humes, J. L. Lipoxygenase pathways of macrophages. *Fed. Proc.* **44:**2933–2936; 1985.
[15] Sevanian, A.; Wratten, M. L.; McLeod, L. L.; Kim, E. Lipid peroxidation and phospholipase A2 activity in liposomes composed of unsaturated phospholipids: a structural basis for enzyme activation. *Biochim. Biophys. Acta* **961:**316–327; 1988.
[16] Evans, M. V.; Turton, H. E.; Grant, C. M.; Dawes, I. W. Toxicity of linoleic acid hydroperoxide to Saccharomyces cerevisiae: involvement of a respiration-related process for maximal sensitivity and adaptive response. *J. Bacteriol.* **180:**483–490; 1998.
[17] Wang, G.; Hong, Y.; Johnson, M. K.; Maier, R. J. Lipid peroxidation as a source of oxidative damage in Helicobacter pylori: protective roles of peroxiredoxins. *Biochim. Biophys. Acta* **1760:**1596–1603; 2006.
[18] Jaeger, T.; Budde, H.; Flohe, L.; Menge, U.; Singh, M.; Trujillo, M.; Radi, R. Multiple thioredoxin-mediated routes to detoxify hydroperoxides in *Mycobacterium tuberculosis*. *Arch. Biochem. Biophys.* **423:**182–191; 2004.
[19] Hu, Y.; Coates, A. R. Acute and persistent Mycobacterium tuberculosis infections depend on the thiol peroxidase TpX. *PLoS One* **4:**e5150; 2009.
[20] Master, S. S.; Springer, B.; Sander, P.; Boettger, E. C.; Deretic, V.; Timmins, G. S. Oxidative stress response genes in Mycobacterium tuberculosis: role of ahpC in resistance to peroxynitrite and stage-specific survival in macrophages. *Microbiology* **148:**3139–3144; 2002.
[21] Manca, C.; Paul, S.; Barry III, C. E.; Freedman, V. H.; Kaplan, G. Mycobacterium tuberculosis catalase and peroxidase activities and resistance to oxidative killing in human monocytes in vitro. *Infect. Immun.* **67:**74–79; 1999.
[22] Zhang, Y.; Heym, B.; Allen, B.; Young, D.; Cole, S. The catalase-peroxidase gene and isoniazid resistance of Mycobacterium tuberculosis. *Nature* **358:**591–593; 1992.
[23] Sherman, D. R.; Mdluli, K.; Hickey, M. J.; Arain, T. M.; Morris, S. L.; Barry III, C. E.; Stover, C. K. Compensatory ahpC gene expression in isoniazid-resistant Mycobacterium tuberculosis. *Science* **272:**1641–1643; 1996.
[24] Jaeger, T. Peroxiredoxin systems in mycobacteria. *Subcell. Biochem.* **44:**207–217; 2007.
[25] Gu, S.; Chen, J.; Dobos, K. M.; Bradbury, E. M.; Belisle, J. T.; Chen, X. Comprehensive proteomic profiling of the membrane constituents of a Mycobacterium tuberculosis strain. *Mol. Cell. Proteomics* **2:**1284–1296; 2003.
[26] Oliva, M.; Theiler, G.; Zamocky, M.; Koua, D.; Margis-Pinheiro, M.; Passardi, F.; Dunand, C. PeroxiBase: a powerful tool to collect and analyse peroxidase sequences from Viridiplantae. *J. Exp. Bot.* **60:**453–459; 2009.
[27] Soito, L.; Williamson, C.; Knutson, S. T.; Fetrow, J. S.; Poole, L. B.; Nelson, K. J. PREX: PeroxiRedoxin classification indEX, a database of subfamily assignments across the diverse peroxiredoxin family. *Nucleic Acids Res.* **39:**D332–D337 (database issue); 2010.
[28] Murphy, D. J.; Brown, J. R. Identification of gene targets against dormant phase Mycobacterium tuberculosis infections. *BMC Infect. Dis.* **7:**84; 2007.
[29] Li, S.; Peterson, N. A.; Kim, M. Y.; Kim, C. Y.; Hung, L. W.; Yu, M.; Lekin, T.; Segelke, B. W.; Lott, J. S.; Baker, E. N. Crystal structure of AhpE from Mycobacterium tuberculosis, a 1-Cys peroxiredoxin. *J. Mol. Biol.* **346:**1035–1046; 2005.
[30] Hugo, M.; Turell, L.; Manta, B.; Botti, H.; Monteiro, G.; Netto, L. E.; Alvarez, B.; Radi, R.; Trujillo, M. Thiol and sulfenic acid oxidation of AhpE, the one-cysteine peroxiredoxin from Mycobacterium tuberculosis: kinetics, acidity constants, and conformational dynamics. *Biochemistry* **48:**9416–9426; 2009.
[31] Trujillo, M.; Clippe, A.; Manta, B.; Ferrer-Sueta, G.; Smeets, A.; Declercq, J. P.; Knoops, B.; Radi, R. Pre-steady state kinetic characterization of human peroxiredoxin 5: taking advantage of Trp84 fluorescence increase upon oxidation. *Arch. Biochem. Biophys.* **467:**95–106; 2007.
[32] Manta, B.; Hugo, M.; Ortiz, C.; Ferrer-Sueta, G.; Trujillo, M.; Denicola, A. The peroxidase and peroxynitrite reductase activity of human erythrocyte peroxiredoxin 2. *Arch. Biochem. Biophys.* **484:**146–154; 2009.

[33] Ogusucu, R.; Rettori, D.; Munhoz, D. C.; Netto, L. E.; Augusto, O. Reactions of yeast thioredoxin peroxidases I and II with hydrogen peroxide and peroxynitrite: rate constants by competitive kinetics. *Free Radic. Biol. Med.* **42:**326–334; 2007.
[34] Parsonage, D.; Karplus, P. A.; Poole, L. B. Substrate specificity and redox potential of AhpC, a bacterial peroxiredoxin. *Proc. Natl Acad. Sci. U. S. A.* **105:**8209–8214; 2008.
[35] Trindade, D. F.; Cerchiaro, G.; Augusto, O. A role for peroxymonocarbonate in the stimulation of biothiol peroxidation by the bicarbonate/carbon dioxide pair. *Chem. Res. Toxicol.* **19:**1475–1482; 2006.
[36] Maskrey, B. H.; Bermudez-Fajardo, A.; Morgan, A. H.; Stewart-Jones, E.; Dioszeghy, V.; Taylor, G. W.; Baker, P. R.; Coles, B.; Coffey, M. J.; Kuhn, H.; O'Donnell, V. B. Activated platelets and monocytes generate four hydroxyphosphatidylethanolamines via lipoxygenase. *J. Biol. Chem.* **282:**20151–20163; 2007.
[37] Pryor, W. A.; Castle, L. Chemical methods for the detection of lipid hydroperoxides. *Methods Enzymol.* **105:**293–299; 1984.
[38] Ellman, G. L. Tissue sulfhydryl groups. *Arch. Biochem. Biophys.* **82:**70–77; 1959.
[39] Trujillo, M.; Radi, R. Peroxynitrite reaction with the reduced and the oxidized forms of lipoic acid: new insights into the reaction of peroxynitrite with thiols. *Arch. Biochem. Biophys.* **397:**91–98; 2002.
[40] Jiang, Z. Y.; Hunt, J. V.; Wolff, S. P. Ferrous ion oxidation in the presence of xylenol orange for detection of lipid hydroperoxide in low density lipoprotein. *Anal. Biochem.* **202:**384–389; 1992.
[41] Jiang, Z. Y.; Woollard, A. C.; Wolff, S. P. Lipid hydroperoxide measurement by oxidation of Fe^{2+} in the presence of xylenol orange: comparison with the TBA assay and an iodometric method. *Lipids* **26:**853–856; 1991.
[42] Humphrey, W.; Dalke, A.; Schulten, K. VMD: visual molecular dynamics. *J. Mol. Graphics* **14:**33–38 27–28; 1996.
[43] Richardson, W. H.; Hodge, V. F. Acidities of tertiary alkyl hydroperoxides. *J. Org. Chem.* **35:**4012–4016; 1970.
[44] Richardson, S. E.; Yao, H.; Frank, K. M.; Bennet, D. A. Equilibria, kinetics and mechanisms in the bicarbonate activation of hydrogen peroxide: oxidation of sulfides by peroxymonocarbonate. *J. Am. Chem. Soc.* **122:**1729–1739; 2000.
[45] Davies, D. M.; Jones, P.; Mantle, D. The kinetics of formation of horseradish peroxidase compound I by reaction with peroxobenzoic acids: pH and peroxo acid substituent effects. *Biochem. J.* **157:**247–253; 1976.
[46] Winterbourn, C. C.; Metodiewa, D. Reactivity of biologically important thiol compounds with superoxide and hydrogen peroxide. *Free Radic. Biol. Med.* **27:** 322–328; 1999.
[47] Hall, A.; Parsonage, D.; Poole, L. B.; Karplus, P. A. Structural evidence that peroxiredoxin catalytic power is based on transition-state stabilization. *J. Mol. Biol.* **402:** 194–209; 2010.
[48] Perrin, D. Ionisation constants of inorganic acids and bases in aqueous solution. IUPAC Chemical Data Series. Pergamon Press, Oxford; 1984.
[49] Ali, S. T.; Karamat, S.; Kona, J.; Fabian, W. M. Theoretical prediction of pK(a) values of seleninic, selenenic, sulfinic, and carboxylic acids by quantum-chemical methods. *J. Phys. Chem. A* **114:**12470–12478; 2010.
[50] Ursini, F.; Maiorino, M.; Gregolin, C. The selenoenzyme phospholipid hydroperoxide glutathione peroxidase. *Biochim. Biophys. Acta* **839:**62–70; 1985.
[51] Soonsanga, S.; Lee, J. W.; Helmann, J. D. Oxidant-dependent switching between reversible and sacrificial oxidation pathways for Bacillus subtilis OhrR. *Mol. Microbiol.* **68:**978–986; 2008.
[52] Declercq, J. P.; Evrard, C.; Clippe, A.; Stricht, D. V.; Bernard, A.; Knoops, B. Crystal structure of human peroxiredoxin 5, a novel type of mammalian peroxiredoxin at 1.5 A resolution. *J. Mol. Biol.* **311:**751–759; 2001.
[53] Piñeyro, M. D.; Arcari, T.; Robello, C.; Radi, R.; Trujillo, M. Tryparedoxin peroxidases from *Trypanosoma cruzi:* high efficiency in the catalytic elimination of hydrogen peroxide and peroxynitrite. *Arch. Biochem. Biophys.* **507:**287–295; 2011.
[54] Bryk, R.; Griffin, P.; Nathan, C. Peroxynitrite reductase activity of bacterial peroxiredoxins. *Nature* **407:**211–215; 2000.
[55] Akaki, T.; Tomioka, H.; Shimizu, T.; Dekio, S.; Sato, K. Comparative roles of free fatty acids with reactive nitrogen intermediates and reactive oxygen intermediates in expression of the anti-microbial activity of macrophages against Mycobacterium tuberculosis. *Clin. Exp. Immunol.* **121:**302–310; 2000.